

Spin–orbit resonance, transit duration variation and possible secular perturbations in KOI-13

Gy. M. Szabó^{1,2*}, A. Pál^{1,3}, A. Derekas¹, A. E. Simon^{1,2}, T. Szalai⁴, L. L. Kiss^{1,5}

¹*Konkoly Observatory of the Hungarian Academy of Sciences, PO. Box 67, H-1525 Budapest, Hungary*

²*Department of Experimental Physics and Astronomical Observatory, University of Szeged, H-6720 Szeged, Hungary*

³*Department of Astronomy, Eötvös University, Pázmány Péter sétány 1/A, 1117 Budapest, Hungary*

⁴*Department of Optics and Quantum Electronics, University of Szeged, Dóm tér 9., H-6720 Szeged, Hungary*

⁵*Sydney Institute for Astronomy, School of Physics A28, University of Sydney, NSW 2006, Australia*

Accepted Received; in original form

ABSTRACT

KOI-13 is the first known transiting system exhibiting light curve distortions due to gravity darkening of the rapidly rotating host star. In this paper we analyse publicly available *Kepler* Q2–Q3 short-cadence observations, revealing a continuous light variation with a period of $P_{\text{rot}} = 25.43 \pm 0.05$ hour and a half-amplitude of 21 ppm, which is linked to stellar rotation. This period is in exact 5:3 resonance with the orbit of KOI-13.01, which is the first detection of a spin-orbit resonance in a host of a substellar companion. The stellar rotation leads to stellar oblateness, which is expected to cause secular variations in the orbital elements. We indeed detect the gradual increment of the transit duration with a rate of $(1.14 \pm 0.30) \times 10^{-6}$ day/cycle. The confidence of this trend is $3.85\text{-}\sigma$, the two-sided false alarm probability is 0.012%. We suggest that the reason for this variation is the expected change of the impact parameter, with a rate of $db/dt = -0.016 \pm 0.004/\text{yr}$. Assuming $b \approx 0.25$, KOI-13.01 may become a non-transiting object in 75 – 100 years. The observed rate is compatible with the expected secular perturbations due to the stellar oblateness yielded by the fast rotation.

Key words: planetary systems

1 INTRODUCTION

KOI-13 (KIC 009941662) is a unique astrophysical laboratory of close-in companions in an oblique orbital geometry. The system consists of a widely separated common proper motion binary of A-type stars, one hosting a highly irradiated planet candidate with $P_{\text{orb}} \approx 1.7626$ day (Borucki 2011). The host star of KOI-13.01 is the brighter component, KOI-13 A, and rotates rapidly ($v \sin i \approx 65 - 70$ km/s, Szabó et al. 2011). The transit curves show significant distortion that is stable in shape, and it is consistent with a companion orbiting a rapidly rotating star exhibiting gravity darkening by rotation (Barnes 2009). Barnes et al. 2011 derived a projected alignment of $\lambda = 23^\circ \pm 4^\circ$ and the star’s north pole is tilted away from the observer by $\psi = 48^\circ \pm 4^\circ$, therefore the stellar inclination, $i_* = 43^\circ \pm 4^\circ$ (assuming $M_* = 2.05 M_\odot$). The mutual inclination is $\varphi = 54\text{--}56^\circ$. Companion is determined to have a mass of $9.2 \pm 1.1 M_J$ (Shporer et al. 2011) and between $4 \pm 2\text{--}6 \pm 3 M_J$ (Mazeh et al. 2011), and a radius of $1.44 R_J$ (Barnes et al. 2011).

On 23 September, 2011, new *Kepler* photometry (Short Cadence Q3 data) became available. Here we suggest that the photometric data reveal the stellar rotation, and give observational evidence for transit duration variations (TDV) which are a sign of secular perturbations.

2 ROTATION OF THE HOST STAR

After removing the orbital phase-dependent light variations from the *Kepler* photometry of KOI-13, we detected an additional periodic signal that we argue below is due to rotation of the host star. The light curve was corrected with a dilution factor of 1.818 (Szabó et al. 2011). The folded light curve with P_{orb} is plotted in the upper panel of Fig. 1 and we see the ellipsoidal and beaming variations (Mazeh et al. 2011, Shporer et al. 2011). The reference flux value is taken to be the centre of the secondary eclipse, when only KOI-13 A is visible. We smoothed and subtracted this variation from the out-of-transit light curve, and de-projected the residuals into the time domain (upper middle panel). A prominent frequency was detected in these residuals at 0.9437 1/day, i.e. at 25.43 ± 0.05 hour period (Fig. 1, lower middle panel).

* E-mail: szgy@konkoly.hu

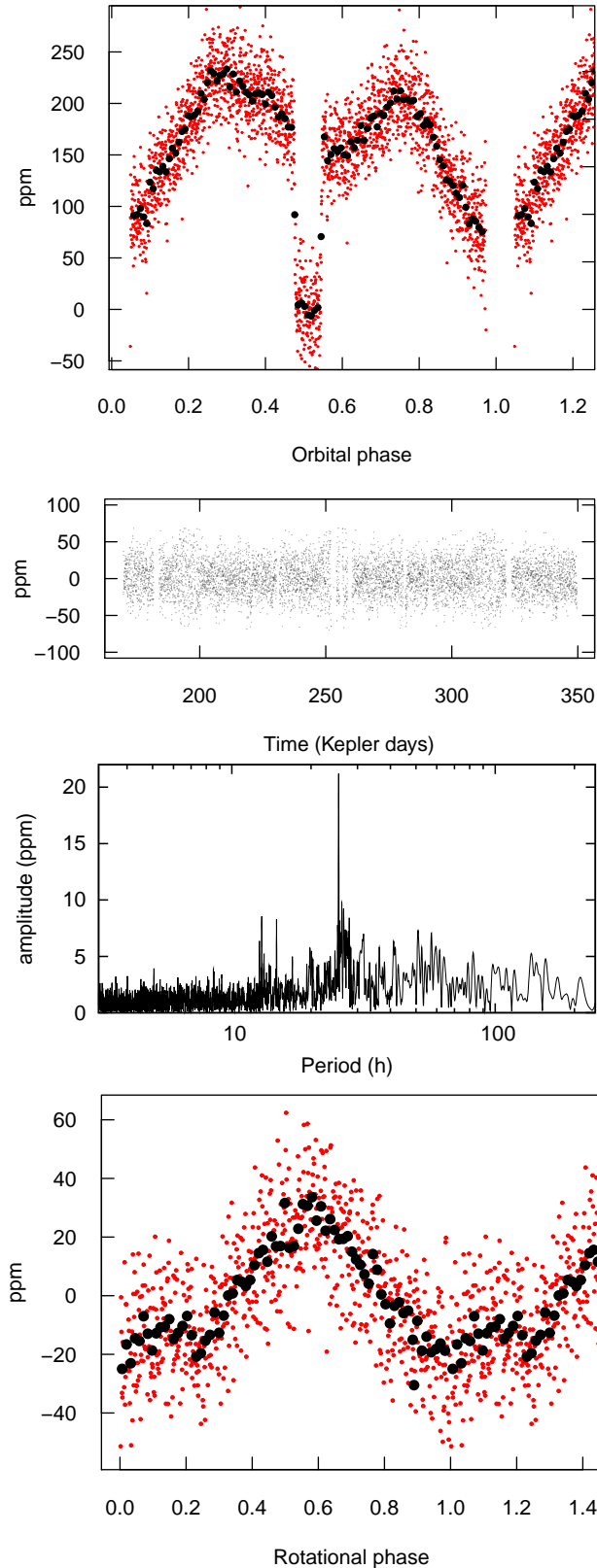


Figure 1. Top: out-of-transit light curve of KOI-13, corrected for the third light. The reference flux level is KOI-13 A, i.e. the flux measured at eclipse. After subtracting this signal from the time series (middle upper panel), a signal with 25.432 hour period is detected with high significance (lower middle panel). Bottom: The phase diagram with 25.432 h period, after removing the orbit-dependent variations.

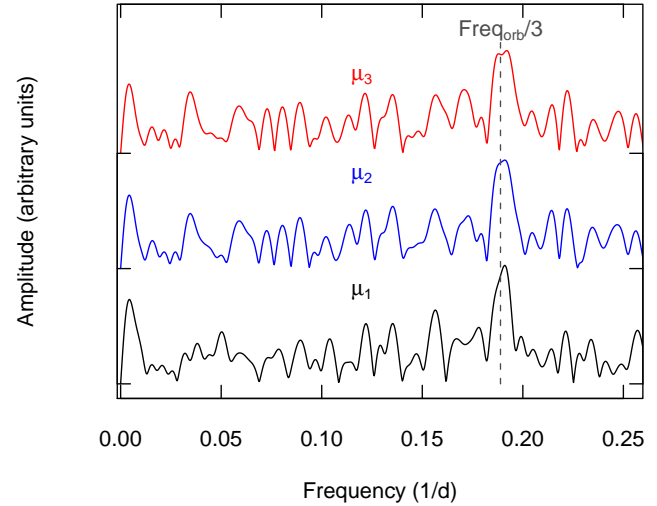


Figure 2. Fourier-transforms of the light curve shape moments μ_1 – μ_3 show modulations in the transit shape with a period of $3P_{\text{orb}}$. The peaks around 0.189 1/day frequency ($= 1/P_{\text{orb}}/3$) have $\approx 4\text{-}\sigma$ confidence.

The semi amplitude of this variation is 21 ppm, well above the average noise level of 1 ppm in the Fourier spectrum. Harmonics of this frequency can also be detected up to the fourth order. This period has been found by Shporer et al. 2011 and Mazeh et al. 2011 independently. The binned phase diagram of the residuals with 25.43 hour period is plotted in the bottom panel of Fig. 1.

Both Mazeh et al (2011) and Shporer et al (2011) suggested a probable pulsational origin. Contrary to their proposition, we interpret it as the rotational period of KOI-13 A. The arguments for a rotational origin are the following:

- The period is perfectly compatible with the expected rotational rate. Barnes et al. 2011 predicted a 22–22.5 hour rotational period for KOI-13 A, depending on the stellar mass. They did not estimate the error, but it is easy to calculate that errors in $v \sin i$ and in the stellar inclination results in ± 3.9 hours. This prediction is in good agreement with the rotational origin of the new period.

- Balona (2011) detected signs of stellar rotation in 20% of all A–F stars in the Kepler field caused by the granulation noise, and 8% of them also exhibit starspot-like features in the light curves. Typically, these stars exhibit a dominant peak with 10–100 ppm amplitude at periods less than 3 days, the median is around 1 day for stars in the range of 7500–10,000 K. Another diagnostic is the scatter level at frequencies below $< 50/\text{day}$, which exponentially increases by a factor of ≈ 1.6 toward low frequencies/high periods. The periodogram of KOI-13 looks exactly as described by Balona (2011), and the folded light curve (Fig. 1, lower panel) is also compatible with a rotating A-type star with magnetic activity.

- Stars similar to KOI-13 A can exhibit p or g mode pulsations (δ Sct and γ Dor) or both (Uytterhoeven et al. 2011). However, the observed pulsations have periods less than one day, and several modes are observed with similar amplitudes. The general appearance of the frequency spectrum of KOI-13 does not resemble a pulsating star.

• Mazeh et al 2011 detected four harmonics of the 25.4-hour frequency in Q3 data, which we confirm here. The presence of such harmonics is typical for stellar rotation (Balona et al. 2011).

It should be noted that both we and Mazeh et al. 2011 detected other frequencies between 1.5–2 c/day which are separated about equidistantly and have amplitudes of 4–7 ppm. Their harmonics do not appear in Q2+Q3 data, and these peaks do look compatible with pulsation.

The source of the 25.4-hour period is the host star, KOI-13 A. This is seen from the systematic modulation of the transit shapes. Because this period is in 3:5 ratio with the orbital period, every third transit occurs in front of the same stellar surface, and a modulation of the light curve shape is expected with a period of 3 transits. Since the individual light curves are too noisy for a direct comparison, we have to combine many data points and analyse their moments. Let us define μ_n , the n -th light curve moment of each individual transit as

$$\mu_n := \sum_{i \in \{\text{transit}\}} \left(\frac{t_i - C_i}{D} \right)^n \Delta f_i \quad (1)$$

where t_i and f_i are the times and occulted fluxes belonging to each data points, D is the transit duration and C_i is the calculated mid-time of the transit, based on the ephemeris in Borucki 2011. Once the moments are assigned to the individual transits, a time series of moments can be analyzed in the standard fashion. In Fig. 2, we plot the periodograms of the first three lightcurve moments (note that the amplitudes are in relative units). The periodograms show a detection with 5.27 day period, with a significance of $3 - 4\sigma$ for each light curve moments, confirming that the 25.4-hour period modulates the shape of the transit with a period of $3P_{orb} = 5P_{rot}$.

2.1 The possible 5:3 spin-orbit resonance of KOI-13 A

The 25.4-hour period is very close (within 0.1%) to the 5:3 spin-orbit resonance with KOI-13.01. Because of the large mutual inclination of 59° (Barnes et al. 2011), the longitude of the companion varies with changing velocity. Interestingly, the synodical longitude of KOI-13.01 remains exactly constant (within 1% fluctuations) on $\approx 1/8$ orbital arc surrounding the positions when the companion is at extremely high/low latitudes. Thus, KOI-13.01 and KOI-13 A move as if they were in exact 1:1 resonance for 3 hours.

To date, theories of spin-orbit resonance cover the following cases: (i) spatial approximation with rigid bodies (e.g. Makarov 2011), where the body in resonance has little mass; (ii): resonant orbits of massive stars (e.g. Witte & Savonije 2011); (iii) resonances in systems of compact bodies (e.g. Schnittman 2004). The case of resonance between the stellar spin and the orbit of a substellar companion is yet to be explored theoretically but, if confirmed, it will be a significant finding in relation to the evolution of planetary systems.

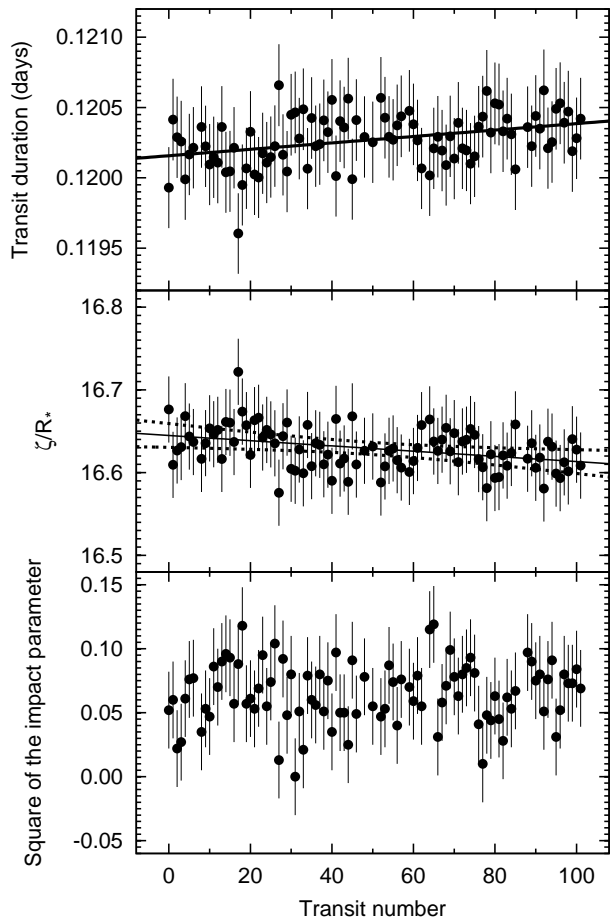


Figure 3. Variations in the transit duration (top panel), the reciprocal transit duration (middle panel) and in the square of the impact parameter derived from transit shape (b^2 , lowest panel), as the function of the cycle number. The plot of the reciprocal transit duration is superimposed by the model of the best-fit linear trend together with the 3σ errors of the linear regression.

3 TRANSIT DURATION VARIATIONS

The analysis of the light curve moments suggested a long-period time-dependent variation in the transit curve shapes. By fitting each transits individually, we concluded that the duration of the transit is gradually increasing (Fig. 3, top panel). The significance of this finding is 3.85σ , with a false alarm probability of 0.012%, based on an MCMC estimate. The 3σ confidence interval of the fitted linear regression is plotted in the middle panel of Fig. 3, onto the distribution of the reciprocal transit length (which is the actual output of the light curve fit algorithm). We now describe the details of how the light curves were analyzed.

First, every transit was fitted independently using the analytic models of Mandel & Agol (2002). This fit invokes symmetric templates which cannot fit the known asymmetry of the light curves; but since the asymmetry appears similarly in each transits, we expect no time-dependent bias in the results. The free model parameters are: the transit time, the relative radius of the planet, the reciprocal of the half duration, ζ/R_* , and the square of the impact parameter, b^2 . These parameters are almost uncorrelated to each other (Pál

2008). Indeed, our analysis shows that the inverse duration ζ/R_* follows a secular trend (see Fig. 3).

The derived values of these parameters are displayed in Fig. 3. Since KOI-13 did not exhibit a transit timing variation, we can rule out short-term secular variations in the orbital semimajor axis of the transiting companion. Therefore, we conclude that the decrease in ζ/R_* , indicating a lengthening of the transit duration, is due to the increasing orbital inclination (i.e. due to decreasing impact parameter). The observed linear trend in ζ/R_* is $d(\zeta/R_*)/dt = (-31.6 \pm 8.2) \cdot 10^{-5} \text{ d}^{-1} \text{ cycle}^{-1} = (-17.9 \pm 4.6) \cdot 10^{-5} \text{ d}^{-2}$. Since the relation between ζ/R_* , a/R_* and b^2 is

$$\left(\frac{a}{R_*}\right) = \frac{\sqrt{1-b^2}}{n} \left(\frac{\zeta}{R_*}\right), \quad (2)$$

(see also Pál 2008), we can compute the time derivative of b as

$$\dot{b} = \frac{db}{dt} = \frac{1-b^2}{b} \left(\frac{\zeta}{R_*}\right)^{-1} \frac{d}{dt} \left(\frac{\zeta}{R_*}\right). \quad (3)$$

This was obtained by re-ordering equation (2) and assuming that a/R_* is constant. By substituting our best-fit $b = 0.253 \pm 0.020$ into this equation, we had $\dot{b} = (-4.4 \pm 1.2) \times 10^{-5} \text{ d}^{-1} = (-0.016 \pm 0.004) \text{ y}^{-1}$. This is a tiny change in the transit duration, an order of magnitude smaller than the precision with which b can be determined from the light curve shape in the fitting procedure (Fig. 3, bottom panel). More precisely, the planet appeared to moved by only $\approx 15\%$ of its radius during the observed ≈ 100 transits, having no detectable effect on the light curve shape. Consequently, we reasonably neglected the oblate shape of the rotating star when converting transit duration to b . The stellar oblateness of a $2 M_\odot$ star with radius $1.7 R_\odot$ is 3% (Murray & Dermott, 1999), and less in an inclined projection. Therefore the bias due to stellar oblateness is 1–2% in the determined value of \dot{b} , much below the accuracy of its determined value. In Section 4, we will show that \dot{b} is compatible with the secular perturbations caused by the oblateness of KOI-13 A, the rotating host star.

4 INTERPRETATION

Assuming $M_p = 9.2 M_J$ (see also Barnes et al. 2011), the angular momentum in the star and the companion are similar. Thus, the axes of both the planet orbit and the stellar spin are precessing around the total angular momentum axis, opposing each other. To date, there is no exact theory for this case. In the observed examples, angular momentum of the orbit (double stars) or stellar spin (e.g. Mercury or lunisolar precession) dominates the other. One can study the precession of the orbital plane and the stellar spin under slightly different assumptions. We will show here that these lead to compatible results, and give a satisfactory estimate of the stellar oblateness.

4.1 Secular J_2 perturbations

As known from the theory of satellite motions (Kaula 1966), higher order moments of the gravitational potential of a host body yield periodic and secular perturbations in the orbits of nearby companions. The external gravitational potential of an extended body can be expressed as

$$V(r, \theta) = -\frac{GM}{R} \left[1 - \sum_{n=2}^{\infty} J_n \left(\frac{R}{r}\right)^n \mathcal{P}_n(\cos \theta) \right], \quad (4)$$

where M is the total mass, R is the equatorial radius, J_n are constants and \mathcal{P}_n are the Legendre polynomials. The most prominent perturbation is caused by J_2 , due to the oblateness of the host body. MacCullagh's Theorem allows us compute J_2 using

$$J_2 = \frac{1}{MR^2} \left(\Theta_{zz} - \frac{\Theta_{xx} + \Theta_{yy}}{2} \right) \approx \frac{\Theta_{zz} - \Theta_{xx}}{MR^2}, \quad (5)$$

where $\Theta_{xx} = \Theta_{yy} \leq \Theta_{zz}$ are the principal moments of inertia. It is known that a non-zero J_2 results in secular perturbations in the angular orbital elements. Namely, the secular term in Ω (argument of ascending node) is computed as

$$\frac{d\Omega}{dt} = -\frac{3}{2} J_2 n \left(\frac{a}{R}\right)^{-2} \frac{\cos \varphi}{(1-e^2)^2}. \quad (6)$$

Here n denotes the orbital mean motion, a is the semi-major axis and e is the orbital eccentricity.

It is known from vector geometry, that if a unit vector \mathbf{n} precesses around the unit vector \mathbf{p} with an angular frequency of ω_0 , the time derivative of \mathbf{n} will be

$$\dot{\mathbf{n}} = \omega_0 (\mathbf{p} \times \mathbf{n}). \quad (7)$$

In our case, \mathbf{n} is the unit vector parallel to the orbital angular momentum of the transiting body. Since the components of \mathbf{n} are

$$\mathbf{n} = \begin{pmatrix} \sin i \cos \Omega \\ \sin i \sin \Omega \\ \cos i \end{pmatrix} \quad (8)$$

and the only observable quantity is $n_z \equiv \cos i$, we can write

$$\dot{n}_z = \omega_0 (p_x n_y - p_y n_x). \quad (9)$$

By substituting $p_x = \sin i_p \cos \Omega_p$ and $p_y = \sin i_p \sin \Omega_p$ and the components n_x and n_y from equation (7), we obtain

$$\frac{d \cos i}{dt} = \omega_0 \sin i \sin i_p \sin \lambda, \quad (10)$$

where Ω_p is the ascending node of the stellar equator, and λ is the longitude of the planet's ascending node, relative to that of the ascending node of the stellar equator by definition.

4.2 The inferred oblateness of the host star

Assuming a circular orbit for the transiting companion and substituting the above relation and equation (??) into equation (6), and by taking $\omega_0 = d\Omega/dt$ as the precession rate induced by J_2 , we finally obtain

$$\begin{aligned} \frac{d \cos i}{dt} &= -\frac{3}{2} J_2 n \left(\frac{a}{R_*}\right)^{-2} \times \\ &\times (\cos i \cos i_p + \sin i \sin i_p \cos \Delta\Omega) \times \\ &\times \sin i \sin i_p \sin \Delta\Omega. \end{aligned} \quad (11)$$

Since transits are observed, we can say here that $\cos i \ll \sin i \approx 1$. In addition, $b = (a/R_*) \cos i$, thus the above equation can be rearranged to give \dot{b} as

$$\dot{b} = -\frac{3}{2} J_2 n \left(\frac{a}{R_*}\right)^{-1} \sin^2 i_p \sin \lambda \cos \lambda. \quad (12)$$

For J_2 we obtain

$$J_2 \sin^2 i_p \sin \lambda \cos \lambda = (3.8 \pm 1.0) \cdot 10^{-5}. \quad (13)$$

Substituting the derived stellar parameters we find $J_2 = (2.1 \pm 0.6) \times 10^{-4}$, and $d\Omega/dt = (3.4 \pm 0.9) \times 10^{-5}/\text{day}$.

Is this result compatible with a model star with the same mass, radius and rotational rate as KOI-13 A? To check this, we calculated the moment of inertia of $n = 3$ polytrope models that were distorted uniform stellar rotation. The distortion of a rotating star is $(R - r)/R = \Omega^2 R^3 (2GM)^{-1} + 3J_2/2$ (Stix 2004), where R and r are the radii at the equator and the poles, respectively. The J_2 term we derived for KOI-13 is two orders of magnitude less than the rotational term and can be neglected. The local distortions were calculated at each internal point and then a z -contraction was applied. We assumed $dz/z = -\Omega^2 r^3 (2GM_r)^{-1} \equiv -3\Omega^2 / (8\pi G \langle \rho \rangle_r)$, where M_r and $\langle \rho \rangle_r$ are the mass and the mean density inside the radius r . This model is a first approximation that neglects higher-order distortions, but is enough precise for a rough estimate because the distortions are everywhere smaller than 3%. The resulting values are $\Theta_{zz} = 0.07760 MR^2$, $\Theta_{xx} = 0.07743 MR^2$, $J_2 = 1.7 \times 10^{-4}$. Thus, the expected value of J_2 is in the range suggested by the theory of secular perturbations, supporting our interpretation.

4.3 Precession rate

Applying the framework developed for lunisolar precession, the precession rate of the star can be formulated as

$$\frac{d\Omega_p}{dt} = \frac{3GM_p(\Theta_{zz} - \Theta_{xx}) \cos \varphi}{2a^3 \Theta_{zz} n} = \frac{3}{2} J_2 \frac{GM_p \cos \varphi}{a^3 n \beta}. \quad (14)$$

Here M_p is the mass of the planet and $\beta = 0.07760$ for KOI-13 A, as we derived in the previous section. Evaluating Eq 14, and applying the value of $J_2 = 2.1 \times 10^{-4}$ we find that $d\Omega_p/dt$ is in the range $(3.81-1.67) \times 10^{-5}/\text{day}$, for a companion of mass between 4–9.2 M_J . Therefore, $d\Omega_p/dt$ has the same order of magnitude that we derived for $d\Omega/dt$. The picture of a planet's plane precessing with ≈ 500 year period, and a star's orbital axis precessing with the same period, is self-consistent for KOI-13.

5 SUMMARY

With high-precision *Kepler* photometry, we detected photometric and dynamical effects of stellar rotation in the exoplanet host KOI-13. From photometry alone, we have detected the following three phenomena for the first time:

- Stellar rotation in a probable resonance with the orbital period of the close-in substellar companion;
- Long-period transit duration variations; and
- Precession of the orbital plane of an exoplanet candidate.

Variations in transit duration were found from the fit of the consecutive light curves to transit shape models. Simultaneously, we fitted other model parameters such as the relative radius of the planet, the impact parameter and the timings of transits, and no variations were found in these quantities. The negative TTV detection is plausible because sec-

ular variations can be detected more easily in TDV than in transit timings for short time coverage (Pál & Kocsis 2008). An argument against the reality of TDV can be that we fitted symmetrical templates to a transit with known slight asymmetry. However, we consider that the detected trend is not an artifact of this kind, because (i) there is no visible time-dependent trend in the asymmetric part of the light curves; (ii) the errors contain the ambiguity introduced by the asymmetric part, while the detection is still significant, and (iii) it is rather unlikely that the varying asymmetries affect only the transit duration, and leave the other parameters unchanged.

In interpreting the cause of transit duration variations, our hypothesis of secular J_2 perturbations is a probable scenario, but other processes cannot be excluded (e.g. perturbations from an unreported outer planet; the presence of a moon around KOI-13.01). However, the stellar rotation is the most plausible reason for TDV, because it does not invoke other bodies into the explanation, and the inferred J_2 is fully compatible with the expected value. In other words, one would predict secular J_2 perturbations of KOI-13.01 at the rate detected, taking into account the rapid rotation of the host star and the close proximity of its substellar companion.

ACKNOWLEDGMENTS

This project has been supported by the Hungarian OTKA Grants K76816, K83790 and MB08C 81013, the ‘‘Lendület’’ Program of the Hungarian Academy of Sciences, the ESA grant PECS 98073 and by the János Bolyai Research Scholarship of the Hungarian Academy of Sciences. Tim Bedding is acknowledged for his comments.

REFERENCES

- Balona, L. A., 2011, MNRAS, 415, 1691
 Balona, L. A. et al., 2011, MNRAS, 413, 2651
 Barnes, J. W., 2009, ApJ, 705, 683
 Barnes, J. W. et al., 2011, ApJS, 197, 10
 Borucki, W. J. et al. 2011, ApJ, 736, 19
 Kaula, W. M.: Theory of satellite geodesy. Applications of satellites to geodesy, Blaisdell, 1966
 Makarov, M., 2011, ApJ, submitted, astro-ph:1110.2658
 Mandel, K. & Agol, E., 2002, ApJ, 580, 171
 Mazeh, T. et al., 2011, in press
 Murray, C. D. and Dermott, S. F., 1999, Solar System Dynamics, Cambridge Univ. Press, Cambridge
 Pál, A. 2008, MNRAS, 390, 281
 Pál, A. & Kocsis, B. 2008, MNRAS, 389, 191
 Pijpers, F. P., 1998, MNRAS, 297, L76
 Schnittman J. D., 2004, PhRvD, 70, 124020
 Shporer, A. et al., 2011, AJ, 142, 195
 Stix, M., 2004, The Sun, Springer-Verlag, Berlin, DE
 Szabó, Gy. M. et al., 2011, ApJ, 736, L4
 Witte M. G., Savonije G. J., 2001, A&A, 366, 840
 Uytterhoeven, K. et al., 2011, A&A, 534, 125